IOPscience iopscience.iop.org

Home Search Collections Journals About Contact us My IOPscience

Structural properties of MgF_2 and ZnS in thin film and in multilayer optical coatings

This content has been downloaded from IOPscience. Please scroll down to see the full text.

2008 J. Phys. D: Appl. Phys. 41 225405

(http://iopscience.iop.org/0022-3727/41/22/225405)

View the table of contents for this issue, or go to the journal homepage for more

Download details:

IP Address: 128.151.150.17
This content was downloaded on 29/06/2017 at 13:59

Please note that terms and conditions apply.

You may also be interested in:

Optical and structural properties of Sb2S3/MgF2 multilayers
F Perales, F Agulló-Rueda, J Lamela et al.

Amorphous to polycrystalline transition in Sb2S3 thin films
F Perales, G Lifante, F Agulló-Rueda et al.

Evolution of the optical and structural properties in ZnS/MgS2 multilayers as the number of layers increases
D Soto, F Perales, G Lifante et al.

Substrate temperature dependent physical properties of In2S3 films
N Revathi, P Prathap, Y P V Subbaiah et al.

Effect of annealing on the structural and optical properties of indium-diffused Cd0.7Zn0.3Se thin films
S D Chavhan, S Senthilarasu, J Lee et al.

Interface smoothing of Mo/Y multilayer mirror
P Gupta, T P Tenka, S Rai et al.

Comparison of different methods for x-ray diffraction line broadening analysis
H Savaloni, M Gholipour-Shahraki and M A Player

Thickness effect on the microstructure, morphology and optoelectronic properties of ZnSfilms
P Prathap, N Revathi, Y P Venkata Subbaiah et al.

Photocatalytic, optical and electrical properties of copper-doped zinc sulfide thin films
S H Mohamed

IOP PUBLISHING JOURNAL OF PHYSICS D: APPLIED PHYSICS

J. Phys. D: Appl. Phys. **41** (2008) 225405 (6pp) doi:10.1088/0022-3727/41/22/225405

Structural properties of MgF_2 and ZnS in thin film and in multilayer optical coatings

F Perales[1], **C de las Heras**[2] **and F Agulló-Rueda**[1]

[1] Instituto de Ciencia de Materiales de Madrid, CSIC, Cantoblanco, E-28049 Madrid, Spain
[2] Departamento de Física de Materiales and Instituto Nicolás Cabrera. Facultad de Ciencias, Universidad Autónoma de Madrid, Cantoblanco, E-28049, Madrid, Spain

Received 10 March 2008, in final form 1 August 2008
Published 29 October 2008
Online at stacks.iop.org/JPhysD/41/225405

Abstract
Different techniques of x-ray diffraction line profile analysis have been used to study the microstructural parameters of the MgF_2 and ZnS thin films as well as MgF/ZnS multilayers. The crystallite size and microstrain of the samples have been estimated from x-ray diffraction by applying Scherrer, Scherrer–Wilson and Williamson–Hall formulae respectively. The effects of thermal annealing at different temperatures on the structure in the material in thin films and in multilayers are studied and compared by the three mentioned relations. Although some different values have been obtained from each expression, the same temperature tendency is observed.

1. Introduction

In recent years there has been growing interest in materials for optical coating applications. Laser performance of solid state media is improved by a coating that protects the faces of the laser diode [1–3]. The coating needs different reflectivities at each facet. The desired reflectivity and its spectral response are obtained by using different multilayer coatings. A dielectric multilayer stack of quarter wave thicknesses of alternately high and low refractive index materials forms a reflection or antireflection coating, respectively. The efficiency of devices is strongly determined by the structural characteristics of the materials in the layers [4–7]. The optical properties of films, such as refractive index, absorption and laser damage threshold, depend largely on the microstructure of the coating such as average grain size, its distribution and orientation in polycrystalline films [8–10]. The film material, substrate temperature and post annealing of the samples can all affect the microstructure. Therefore, some knowledge of the film structure and its temperature variation is required for improving their optical applications. For these reasons an analysis of the XRD peaks by the most common formulae will help to know the variation of the microstructure.

Periodic layered media grown by different techniques have been widely used as optical coatings (1). In previous papers [11, 12] we have presented optical and structural properties of Sb_2S_3 and MgF_2 thin films, respectively, as well as of Sb_2S_3/MgF_2 multilayers [13]. This material has low transmittance in the crystalline phase in the wavelength range 0.12–8.5 μm and therefore, for our optical coating purposes ZnS/MgF_2 shows some advantages. In this paper we present results obtained for MgF_2 and ZnS single layers and ZnS/MgF_2 multilayers grown by thermal evaporation and submitted to thermal annealing. The role of the deposition rate and the substrate temperature on the structure of zinc sulfide and magnesium fluoride has been studied before [14, 15]. These materials are very suitable for optical instrument devices in thin film form. Moreover the changes in the structural properties of these materials when they form thin films and multilayers have not been studied before, to the best of our knowledge.

The microstructure parameters of single and multiple layers were analysed by line profile analysis of x-ray diffraction. The main domain size and microstrains are evaluated, respectively, by applying different fittings. The evolution by thermal treatment post-evaporation of these properties follows.

2. Experimental

MgF_2 and ZnS single layers and MgF_2/ZnS multilayers have been grown by thermal evaporation in an Edward Auto 306 coating system [11]. The system has a four position turret

 © 2008 IOP Publishing Ltd Printed in the UK

source which leads to the evaporation of different materials in an alternating way. The initial materials were granular MgF_2 and ZnS, which were placed for evaporation in their respective molybdenum boats. During the process we can choose for evaporation alternately one source or the other to obtain the multilayers. Substrates were cleaned with ethanol in an ultrasonic bath. They were placed in a rotating sample holder, which is concentric with the material source. All the depositions were made at room temperature, and during the evaporation thickness and velocity deposition were continuously monitored with a quartz microbalance by using a FTM5 monitor. For the monolayers case thicknesses of 1.600 μm for MgF_2 and 1.350 μm for ZnS were obtained. Multilayers of four high–low refraction index periods have been grown. Thicknesses of the films were near 0.120 μm for MgF_2 and 0.070 μm for ZnS, which correspond to a $\lambda/4$ film at a light wavelength of 0.650 μm for both materials. The obtained samples were subjected to annealing at temperatures in the 200–400 °C range for 2 h.

The sample structure was studied at room temperature by x-ray diffractograms (XRD) recorded in a Siemens D5000 difractometer in grazing incidence at 1°, with monochromatized Cu Kα (λ = 1.5418 Å) radiation, working at 40 kV and 30 mA. The angular resolution is 0.001°. A secondary graphite monochromator served to suppress fluorescence. Diagrams were collected in the step scanning mode with a step size $2\theta = 0.02°$ and a count time of 2 s. A mirror and divergent slits were selected to ensure complete illumination.

To observe any structural changes in the crystallites when the annealing temperature increases Raman spectra were taken at room temperature with a Renishaw Ramascope 2000 microspectrometer and an argon ion laser operating at a wavelength of 0.5145 μm as the excitation source. The spectral resolution was 40 mm^{-1}. The laser light was focused on the sample through an optical microscope, keeping the power density on the sample below 10 MW m^{-2} to avoid damage to the films. Scattered light was collected through the same microscope, providing a spatial resolution of about 1 μm.

3. Theory

The crystalline size and microstrain of the thin films and the multilayers have been calculated by Scherrer (S), Scherrer–Wilson (S–W) and Williamson–Hall (W–H) formulae [16].

The Scherrer equation is considered in the limiting case of pure particle size broadening, β_p. In this case, the line width is related to the effective particle size d, the x-ray wavelength, λ, of Cu Kα_1 irradiation and the Bragg angle θ as follows:

$$d = \frac{K\lambda}{\beta_p \cos\theta}. \qquad (1)$$

In general, crystallites in polycrystalline thin films exhibit defects and changes in the crystal lattice parameters. When stress broadening is considered, the breadth is related to the effective strain, $\varepsilon_{rms} = \langle \varepsilon^2 \rangle^{1/2}$, and the Bragg angle by the equation

$$\beta_s = \varepsilon_{rms} \tan\theta.$$

If both types of broadening are present, the resultant line width β must be obtained by adding the broadening due to both contributions, but it has been shown that for the commonly occurring Lorentzian line shape the breadths are additive $\beta = \beta_p + \beta_s$.

In this case we may write

$$\beta \cos\theta = \frac{K\lambda}{d} + 4\varepsilon \sin\theta. \qquad (2)$$

This is like the W–H technique [17], which has also been applied for multilayers [9].

Also, the grain sizes and microstrains can be calculated according to the S–W equation [10] by intrinsic profile deconvolution from data of 2θ positions, Gaussian (to fit microstrain component) and Cauchy (to fit the grain size component). Now the breadths are not linear and the total breadth is given by $\beta^2 = \beta_p^2 + \beta_s^2$, and the equation is

$$\frac{\beta^2}{\tan^2\theta} = \frac{K\lambda}{d}\left(\frac{\beta}{\tan\theta \sin\theta}\right) + 20\langle \varepsilon^2 \rangle, \qquad (3)$$

where λ, β and d have the same meanings as in the above relations and $\langle \varepsilon^2 \rangle$ represent the thickness and the mean lattice strain of the crystallite, respectively.

Therefore, it is necessary to have a family of parallel planes to obtain the grain size and the microstrain by S–W and W–H formulae. These planes are chosen from the XRD spectra. In the Scherrer case an average of the grain size obtained from these planes is plotted.

The different methods do not give the same value for the crystalline size. This is because they each yield different characteristic averages from the crystallite size distribution.

Errors of the values have been calculated for the different expressions. Thus, for the grain size calculated by Scherrer the error is 1 Å, by S–W 30 Å and 80 Å by W–H. For the microstrain, the error values are 0.8×10^{-3} for S–W equation and 2×10^{-3} for W–H. They are not plotted in the figures for clarity.

4. Experimental results

4.1. Magnesium fluoride (MgF_2) thin film

In figure 1 the XRD spectra of samples at different annealing temperatures, where a tetragonal structure of MgF_2 is observed, are shown. From (1 1 0) and (2 2 0) reflections of these spectra the grain size and the microstrain are calculated by equations (1), (2) and (3), respectively. The results are shown in figures 2 and 3. As expected, the increase in the grain size shown in figure 2 is smaller when we apply equation (1), where the broadening of the peaks is attributed only to the particle size. However increases are appreciable if we apply equations (2) and (3).

In figure 3, microstrains are represented by applying equations (2) and (3), respectively, to the reflections (1 1 0) and (2 2 0). A maximum value can be seen at 200 °C and then there is a relaxation of the strain. Below that temperature there

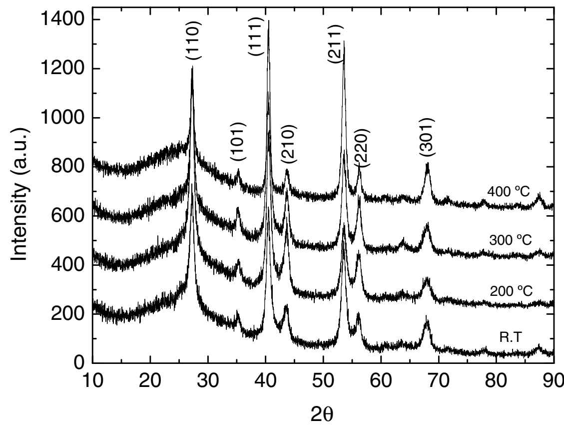

Figure 1. DRX spectra of MgF_2 thin films.

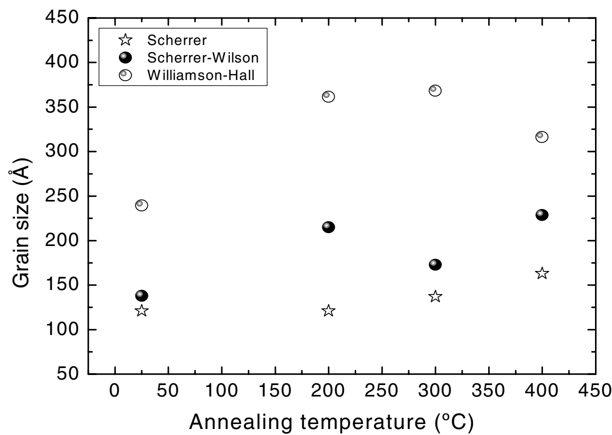

Figure 2. Grain size of MgF_2 calculated from equations (1), (2) and (3).

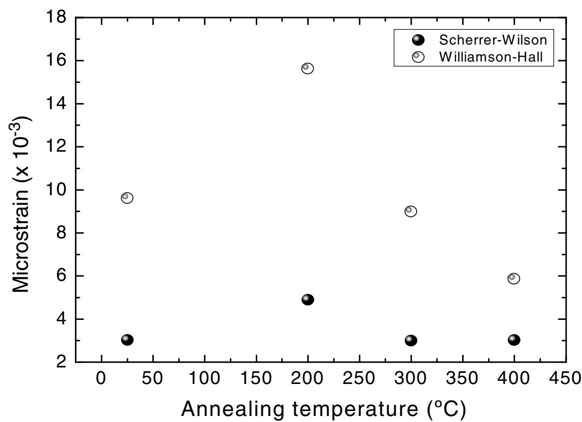

Figure 3. Microstrain of MgF_2 calculated from equations (2) and (3).

are neither grain boundary movements nor defect elimination and for this reason there is a strong increase in the stress due to the increase in the crystallite size. This effect will also be shown in other samples.

Also in figure 3, an appreciable difference between the absolute values for microstrains obtained by S–W and W–H can be observed ($\sim 7 \times 10^{-3}$), although the tendency with the temperature is the same.

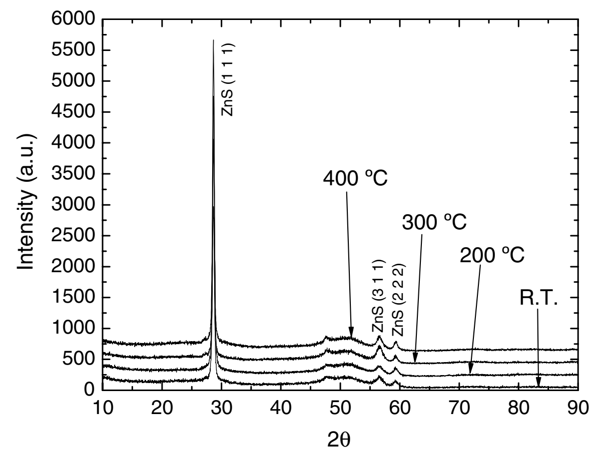

Figure 4. DRX spectra of ZnS thin films.

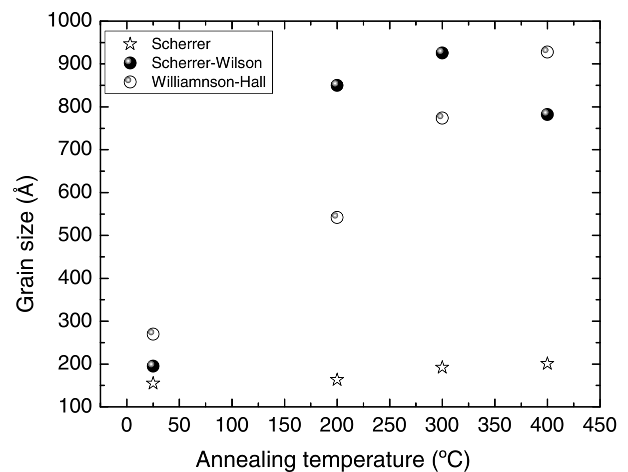

Figure 5. Grain size of ZnS calculated from equations (1), (2) and (3).

4.2. Zinc sulfide (ZnS) thin film

The DRX spectra of this material at different annealing temperatures are shown in figure 4. There, the cubic structure appears with a (1 1 1) preferential direction. As in the MgF_2 case, grain size and microstrain have been obtained by applying equations (1), (2) and (3). With equations (2) and (3), the increases in the ZnS grain size with the highest temperature rise to near 900 nm in that temperature range as can be observed in figure 5. Here also microstrains decrease from 200 °C, as shown in figure 6. Also in MgF_2, different values have been obtained by different fittings. As expected, grain growth is associated with the relaxation of microstrain in the samples.

4.3. Multilayers

The DRX spectra of MgF_2/ZnS multilayers are shown in figure 7, where only peaks from MgF_2 and ZnS appear. There are no peaks corresponding to the mixed combination of these two materials. These spectra have been analysed by equations (1), (2) and (3).

In figure 8, the grain size of MgF_2 layer in the multilayer is plotted. A decrease in the grain size in relation to those

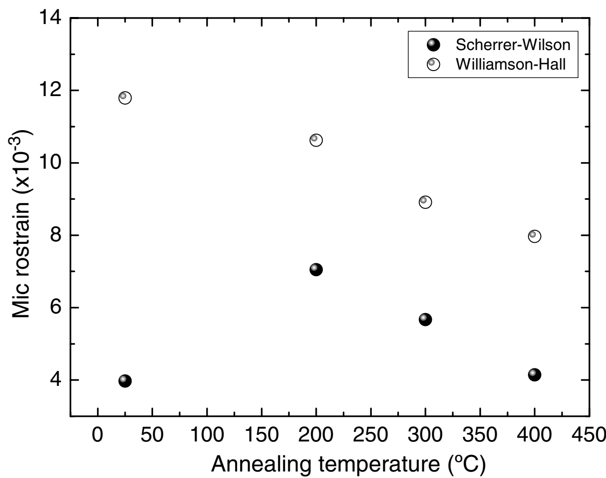

Figure 6. Microstrain ZnS calculated from equations (1), (2) and (3).

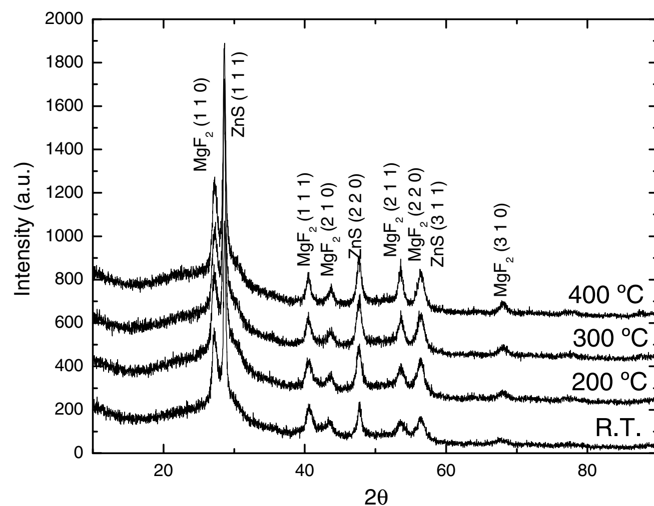

Figure 7. DRX of the multilayers annealed at 200, 300 and 400 °C.

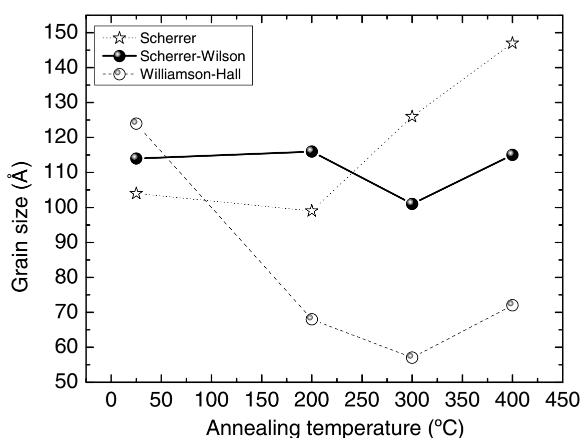

Figure 8. Grain size of MgF_2 in the multilayer.

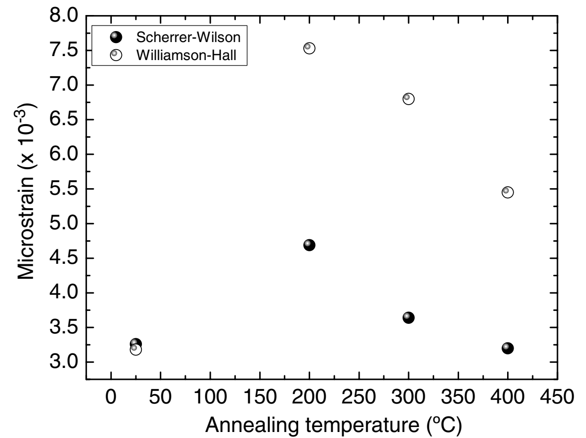

Figure 9. Microstrain of MgF_2 in the multilayer.

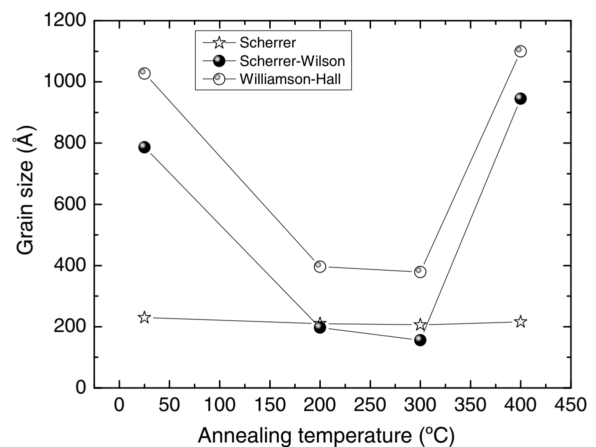

Figure 10. Grain size of ZnS in the multilayer.

obtained for the monolayer in figure 4 is observed for all the fittings. This can be understood by the thickness difference in both samples. However, the tendency with temperature is different. The data obtained by applying the Scherrer equation show an increase with the annealing temperature as in the monolayer. In contrast, those obtained by the W–H indicate a decrease with annealing temperature at the difference with the monolayer, and finally by applying the S–W equation the obtained grain size is nearly constant.

In figure 9, the microstrains calculated by equations (2) and (3) are plotted. A decrease with respect to the values obtained by equation (3) for monolayers is observed for all temperatures. Here there is a coincidence in the values obtained by the two equations in the as-grown sample, but for annealed samples, the microstrains calculated by equation (2) are smaller than those calculated by equation (3), as in the case of monolayers. However, the difference between them is smaller in this case ($\sim 3 \times 10^{-3}$). Otherwise, both equations give the same behaviour with temperature for the microstrains; a maximum appears at 200 °C and then it decreases, as has been seen in thin films. The effect of interface stresses on the average stress in multilayers may be responsible for the difference with thin film values.

The same analysis has been carried out for ZnS in multilayers and is shown in figures 10 and 11.

The Scherrer equation gives a constant grain size. On the other hand, grain size values obtained in the as-grown multilayers by applying equations (2) and (3) are bigger than those obtained for the monolayer, but after annealing,

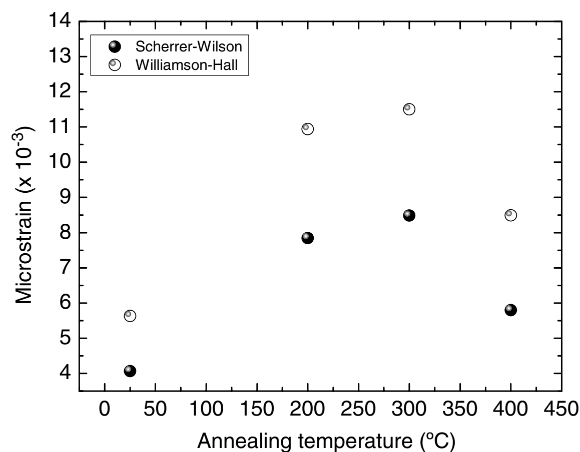

Figure 11. Microstrain of ZnS in the multilayer.

an appreciable decrease is observed at 200 °C and 300 °C, respectively. Here the values tend to adapt to the grain values of MgF_2 in the multilayers. An increase up to the initial values is observed after annealing at 400°C. By applying equations (2) and (3), similar behaviour with temperature for grain size and for microstrains, respectively, is observed. As expected, as the grain size decreases the microstrain increases and vice versa [18–20]. Again there is a maximum of microstrain at 200–300 °C, in coincidence with the minimum observed in grain size.

By annealing at 400 °C the grain size value obtained for ZnS in monolayers is bigger than that in multilayers as expected due to the difference in thicknesses. However, the values of the microstrain are similar. We think that the microstrain may not be due to the grain size, but due to the capacity of moving out of the grain boundaries [21–23]. If the boundaries do not have enough mobility, the microstrains, which originate at the interfaces, will increase instead of relaxing.

Raman spectra have been measured for all the samples. Only the peaks due to MgF_2 appear; the ZnS has a cubic structure that does not show any first order Raman spectrum. The samples were grown with a thickness bigger than 1 μm in order to obtain a good Raman signal. The results show that above 100 °C there is no variation in the wave number when the annealing temperature is increased. Moreover if these results are compared with the spectra of thin MgF_2 films, it is shown that there are no differences above 100 °C. The only difference appears in the spectra at 100 °C for MgF_2 thin film where the peaks due to the structure appear but not for the multilayer at the same temperature. This effect is probably due to the broadening induced by phonon confinement in nanocrystals, because the grain size in multilayers is below 150 Å at this temperature. Spectra are not shown here because they do not show any additional information.

5. Discussion

5.1. Crystallite size

In relation to the obtained results on the crystallite size we can say that the increase in the annealing temperature causes an increase in the crystalline size in both materials MgF_2 and ZnS in thin films and also in multilayer form but this increase is much more pronounced when they are in thin films. This can be observed when we fit the data to all the formulae mentioned above. The values obtained in thin films and in multilayers are different. When they are part of multilayers the total increase is not appreciable or it is negative.

In particular, if we observe MgF_2 thin films by the applied Scherrer formulae, an increase of 25% is observed in the temperature range, the same as when it is a part of a multilayer. However, by the applied S–W an increase of 60% is observed in thin films but little variation with temperature in the multilayer case. By the applied W–H, in thin films the increase is 40% and in multilayers the variation is negative −36%.

In ZnS, different variations are also observed. In this case the differences in the observed values between thin films and multilayers are more pronounced. By Scherrer fitting a 33% increase is observed in thin films and no increase is observed in the same range in multilayers. By the S–W equation the 300% increase observed in thin films is 25% in multilayers. In the same manner, by the W–H equation, the increase of 245% in thin films decreased to 5% in multilayers. It can be mentioned that in both cases, S–W and W–H, the crystalline size in the multilayer case reduces abruptly for intermediate temperatures.

5.2. Microstrain

The difference in the values obtained for the crystalline size by applying the different fittings indicates the importance of the microstrain. Uniformity of behaviour with temperature is observed in thin films and in multilayers: increases of them for the intermediate temperatures and decreases for the highest ones. In all cases, by applying the W–H, the obtained values are higher than by applying S–W. The absolute values are different for thin films and multilayers. In fact, if we observed MgF_2, in thin films, for the temperature interval, microstrain values are in the range (3–5) $\times 10^{-3}$ by S–W and (6–16) $\times 10^{-3}$ by W–H. However in multilayers, the values are (3–4.5) $\times 10^{-3}$ by S–W and (3–7.5) $\times 10^{-3}$ for W–H. This indicates that for MgF_2 microstrain diminishes when it is in multilayers. In the ZnS case microstrain values for thin films are (4–7) $\times 10^{-3}$ for S–W and (12–8) $\times 10^{-3}$ for W–H. For the multilayer case the values of microstrain obtained are (4–8) $\times 10^{-3}$ by S–W and (5–12) $\times 10^{-3}$ for W–H. In this case the values in thin films and in multilayers are very similar.

6. Conclusions

The structural properties of MgF_2 and ZnS thin films and MgF_2/ZnS multilayers grown by PVD have been analysed by three different formulae in all cases. From the Scherrer equation only the crystalline size can be calculated and it shows that it increases with annealing temperature. From the S–W and W–H methods the crystallite size also increases, but much more abruptly, because the contribution of the microstrain to the peak broadening is considered. For both methods the qualitative behaviour of these properties is the same in

monolayer and in multilayers, but the W–H method shows higher values in the crystallite size and in microstrain. In the multilayer case, a tendency of the crystallite size to become similar for the two components has been observed. This has been observed before in other samples (13). The differences observed in values obtained by the different methods may be due to the width of the Bragg reflection being also affected by other distortions of the crystal structure such as dislocations and stacking faults. The crystalline orientation distribution is assumed in many line profile analysis approaches to be a random one. This presupposition is not generally fulfilled in polycrystalline thin films. Preferred orientation or texture is typically observed. The differences in the crystalline size in multilayers and monolayers are due to the difference in thicknesses. Densification of a film constrained by a substrate leads to tensile stresses in the film. The grain boundaries in the film can contribute to densification as sinks for excess vacancies or by eliminating excess boundary volume as a result of grain growth. In multilayers, the interfaces between different materials can contribute to the elimination of stress and as a consequence smaller values are obtained. Finally, in the single layers the Raman spectra show only the peaks for MgF_2. ZnS does not show any peak due to its cubic structure. Comparing the Raman spectra of the MgF_2 thin film and the multilayer there is only one difference for the 100 °C sample, where the multilayer structure does not show Raman peaks, probably because of the small size of the crystallites.

Acknowledgments

This work has been supported by the Spanish Ministerio de Educación y Ciencia under Grant MAT-2004-03347.

References

[1] Macleod H A 2003 *Thin Film Optical Filters* (Bristol: Institute of Physics Publishing)
[2] Martin U 1998 *Annual Report* Department of Optoelectronics, University of Ulm
[3] Hu H, Fan Z and Luo F 2001 *Appl. Opt.* **40** 1950
[4] Ganesha Shanbhogue H *et al* 1998 *Thin Solid Films* **320** 290–7
[5] Sanyal M K *et al* 1998 *Appl. Surf. Sci.* **133** 98–102
[6] Shuzhen S *et al* 2005 *Appl. Surf. Sci.* **249** 157–61
[7] Hass G and Ritter E 1967 *J. Vac. Sci. Technol.* **4** 71
[8] Thompson C V and Carel R 1996 *J. Mech. Phys. Solids* **44** 657
[9] Pelleg J, Elis E and Mogilyanski D 2005 *Met. Mater. Trans.* A **36** 3187
[10] Klug H P and Alexander L E 1974 *X-ray Diffraction Procedures for Polycrystalline and Amorphous Materials* (New York: Wiley Interscience)
[11] Perales F, Herrero J M, Jaque D and de las Heras C 2007 *Opt. Mater.* **29** 783–7
[12] Perales F, Lifante G, Agullo-Rueda F and de las Heras C 2007 *J. Phys. D: Appl. Phys.* **40** 2440–4
[13] Perales F, Agulló-Rueda F, Lamela J and de las Heras C 2008 *J. Phys. D: Appl. Phys* **41** 045403
[14] Al-Douri A A J and Heavens O S 1983 *J. Phys. D: Appl. Phys.* **16** 927
[15] Sharma S K, Yadava V N and Chopra K L 1974 *Japan. J. Appl. Phys. Suppl.* **2** 685
[16] Birkholz M 2006 *Thin Film Analysis by X-ray Scattering* (New York: Wiley-VCH)
[17] Williamson G K and Hall W H 1953 *Acta Metall.* **1** 22
[18] Ghosh C *et al* 1974 *J. Phys. D: Appl. Phys.* **7** 1773–7
[19] Vedeshwar A G 1996 *J. Phys. III France* **5** 1161–72
[20] Tigau N *et al* 2002 *J. Optoelectron. Adv. Mater.* **4** 943–8
[21] Chaudhari P 1972 *J. Vac. Sci. Technol.* **9** 520
[22] Gumbsch P and Daw M 1991 *Phys. Rev.* B **44** 6243
[23] Spaepen F 2000 *Acta Mater.* **48** 31